MODELING OF FLOW INTERACTION OF A LIQUID JET WITH A CONTAMINANT DROPLET

Lang-Mann Chang
Computational Interior Ballistics Branch
Interior Ballistics Division
US Army Ballistic Research Laboratory, ARRADCOM
Aberdeen Proving Ground, Maryland 21005

ABSTRACT. Two flow models have been developed for investigation of the flow interaction of a liquid jet with a chemical contaminant droplet on a plane wall. This interaction is considered as a two-dimensional viscous flow problem. Computer plots are presented for the flow pattern and the evolution of the droplet upon jet impingement. Displacements and mean velocity of the droplet upstream edge are provided as functions of jet velocity and fluid viscosity. These values may be used for evaluation of the efficiency of jet impingement for decontamination. Typical instantaneous pressure distribution on the impingement wall is also given. Studies in progress will establish correlations between flow parameters, such as the incidence angle and the diameter of the jet, and the performance of jet impingement.

I. INTRODUCTION. The present investigation involves utilization of jet impingement for chemical decontamination. The procedure is to use the great force produced by the impingement of jets to remove chemical contaminant droplets from surfaces of a vehicle or equipment.

While falling through air, the contaminant droplets assume the shape of rain drops, with diameters ranging from 1 mm to 2 mm. After impact on a flat surface, each droplet may spread out to 2 - 4 mm in diameter and the average number density of droplets in a surface area of 10 cm by 10 cm is 4.2. Its viscosity may vary widely from 10 to 1000 times that of plain water primarily depending on the temperature.

If not removed, the contaminant may gradually penetrate into the surface and become permanent residue or after drying out may appear as a stain on the surface. A hazardous environment still exists. Of various methods proposed for removal of the contaminant, utilization of liquid jets appears to be the most effective and perhaps most economical at the current level of technological development. The liquid jet can easily break up the droplets and subsequently carry away the contaminant. A thorough clean-up of the surface can be achieved by moving the jet toward the contaminant droplets.

The task seems to be as simple as using a sink hose spray to wash a dish. However, little has been known about the flow interaction of the individual jets in the spray with the dirt droplets on the dish and about the effects of varying a flow parameter, such as the incidence angle of the jet, on the performance of the spray. In the battlefield, in particular, the supply of jet fluid as well as the power source for the pumping system could be very limited. As a result, the efficiency of the jet system in terms of decontaminating a larger area with least consumption of jet fluid and with shortest period of time to complete the mission is of great concern.

In the design of an highly efficient jet system, the following knowledge is vital: the general flow pattern, the evolution of the contaminant droplet, and the effect of varying each flow parameter on the flow. Though this information can be sought via experiments, the work will need very sophisticated instrumentation and will be very costly. As an alternative, computer simulations based on appropriate flow models will be a more desirable means. In fact, the method can provide much greater flexibility for examining areas of importance in the flow field and the results can provide better insights into flow phenomena. The computer results then can be checked by sample experiments for accuracy.

The present jet-contaminant flow consists of two fluids, namely the jet fluid and the contaminant, or three fluids if the ambient is treated as the third one. The two prime fluids are separated by interfaces and have free surfaces with the ambient. The flow is three-dimensional in nature and is highly transient. Much research work has been done in the past on jet impingement problems. However, very few involve a second fluid interacting with the jet in the impingement region. Historically, Taylor [1] remarked that in 1890 Michell [2] gave a solution for the pressure distribution on a flat plate when subjected to a two-dimensional, steady, incompressible, inviscid jet impingement. Nevertheless, it was not known how the solution was obtained until Taylor himself derived an expression for the pressure distribution. In recent years, most of the work in this area is relevant to the VTOL program (vertical takeoff and landing air craft) and are concentrated in impingements on a solid surface. Among them, Scholtz and Trass [3] and Rubell [4,5] considered two- and three-dimensional inviscid, normal and oblique impingements. Their analytical solutions of the surface pressure were, in general, in good agreement with experimental data. In another development which included viscous and turbulence effects, Kotansky and Bower [6] used incompressible Reynolds equations with a one-equation turbulence model to calculate the surface pressure upon a two-dimensional normal impingement. Most recently, Bower [7] extended the problem to three dimensions and used the popular Jones-Lauder two-equation turbulence model [8] for surface pressure and velocity predictions. The results compared reasonably well with measurements. For impingements on a liquid surface, Hunt [9] and Vanden-Broeck [10] treated the problem as a steady and two-dimensional one and used simplified theories to characterize the wave-like hydrodynamic instability occurring at the interface of the two fluids. All of the papers cited above were dealing with steady-state flows and no analyses were given for velocity and pressure distributions when a second fluid was present in the impingement region.

In the present investigation, we have simplified the jet-contaminant flow by treating it as a two-dimensional problem. We have developed a two-fluid flow model and a one-fluid flow model suitable for characterizing the interaction flows developing from two different pre-impingement flow configurations. The unsteady Navier-Stokes equations have been used to describe the flow and the computer code SOLA-VOF [11] has been employed for numerical solutions. Presented are the flow pattern, evolution of the contaminant droplet, effects of variation of flow parameters on the flow, and some typical pressure distributions on the impingement surface.

II. FLOW MODELS. Two configurations can be considered to describe the pre-impingement flow situations occurring in the decontamination process. In

the first configuration, as depicted in Figure 1a, a water jet is directed at a contaminant droplet which is at rest on a surface. In the second configuration, Figure 1b, the contaminant droplet is covered by a water layer which is stationary or flowing. In both cases the impingement flow developed is a three-dimensional problem involving two fluids (contaminant and water) interacting in a region open to the ambient. There exist interfaces separating the two fluids and each of them may have free surfaces with the ambient. Methods for solving such a complex problem are not well developed.

In order to simplify the analysis we will develop one-fluid and two-fluid flow models suitable for characterizing the flows developing from the above two configurations and also suitable for utilizing the computer code SOLA-VOF [11] for solutions. Both models describe a two-dimensional viscous flow. It is noted that the computer code is capable of solving flow problems of two fluids separated by interfaces in a region without voids or one fluid having voids (the ambient).

For the two-fluid model, we establish a two-dimensional channel-type flow shown in Figure 2. It is essentially a flow region covering the major part of the flow shown in Figure 1b. The channel contains two fluids, the contaminant and water which fills the rest of the channel. The upper wall of the channel coincides with the upper free surface of the water layer so as to eliminate consideration of the free surfaces. An outflow boundary condition is specified at this wall and at the ends of the channel, allowing the fluids to flow out the region. The contaminant which covers a rectangular region is assumed to wet perfectly the lower wall of the channel. To account for viscous effects, a no-slip condition is used for the lower wall. We adapt a finer mesh near the wall in order to provide better solutions in thin viscous layers. Finally, a steady uniform jet velocity is specified along a section of the upper wall.

For the one-fluid flow model, we establish a flow region shown in Figure 3, in which the contaminant and the water are assumed to have the same physical properties. In addition, the flow model differs from the two-fluid flow model in that the water initially filling in the channel is absent and there is an initial setup for the jet profile inside the channel. After the flow is initiated, the boundary conditions are identical for both flow models. In the one-fluid flow model, there are only free surfaces, but no interfaces, involved. This model is suitable for characterizing the flow developing from the configuration shown in Figure 1a for which the two-fluid flow model is not applicable because of the existence of both interfaces and free surfaces and, thus, beyond the capability of the SOLA-VOF code. The validity of the one-fluid model will be discussed in Section IV of this paper.

III. FLOW EQUATIONS AND METHOD OF SOLUTION. The governing equations for the model flow are:

continuity
$$\frac{1}{\rho c^2}\frac{\partial p}{\partial t} + \frac{\partial u}{\partial x} + \frac{\partial v}{\partial y} = 0 \qquad (1)$$

momentum
$$\frac{\partial u}{\partial t} + u\frac{\partial u}{\partial x} + v\frac{\partial u}{\partial y} = -\frac{1}{\rho}\frac{\partial p}{\partial x} + \nu\left[\frac{\partial^2 u}{\partial x^2} + \frac{\partial^2 u}{\partial y^2}\right] \qquad (2)$$

$$\frac{\partial v}{\partial t} + u\frac{\partial v}{\partial x} + v\frac{\partial v}{\partial y} = -\frac{1}{\rho}\frac{\partial p}{\partial y} + \nu\left[\frac{\partial^2 v}{\partial x^2} + \frac{\partial^2 v}{\partial y^2}\right] \qquad (3)$$

where t is time variable, u and v are the x-component (along the channel) and the y-component (normal to the channel) of the jet velocity V_j, respectively. The density ρ, the sound speed c, and the viscosity ν, are constant. In addition, a function F, called the fractional volume of fluid function, is introduced for tracking the water-contaminant interface. The function is given as

$$\frac{\partial F}{\partial t} + u\frac{\partial F}{\partial x} + v\frac{\partial F}{\partial y} = 0 \qquad (4)$$

This equation states that F moves with the fluid. In a two-fluid flow the value of F is unity at any point occupied by the first fluid (say, contaminant) and zero elsewhere. When averaged over the cells of a computational mesh, the average value of F in a cell is equal to the fractional volume of the cell occupied by the first fluid. In particular, a unity value of F corresponds to a cell full of the first fluid, whereas a zero value indicates that the cell contains only the second fluid (say, water including the jet fluid and the water layer of Figure 2). Cells with F values between zero and one contain an interface, as illustrated in Figure 4. With this, the interfaces separating the two fluids can be tracked. In the case of one-fluid flow, the second fluid is replaced by the ambient.

The velocity components u and v in the momentum Eqs. (2) and (3) have been solved by using the explicit finite difference scheme, while the pressure p has been computed, coupled with the continuity equation (Eq. (1)) via an implicit finite difference method. The solution of the F function in Eq. (4) has been obtained by using the Donor-Accepter flux approximation. Details of the solution method have been given in Reference 11 of this paper. In order to observe the evolution (location and shape) of the region covered by the contaminant droplet, Marker Particles have been embedded in the fluid and move with it, but do not affect the fluid dynamics.

In the current version of the SOLA-VOF, the viscosities of both fluids in a flow are considered the same or simply zero. To adapt this code for solving the present flow which involves two fluids with very different viscosities the following modification is necessary.

$$\nu = \nu_c F + (1 - F)\,\nu_w \qquad (5)$$

where ν is the kinematic viscosity of fluid in a cell, ν_c the kinematic viscosity of the first fluid (contaminant), ν_w the kinematic viscosity of the second fluid (jet fluid), and F the function defined in Eq. (4). Similarly, if the densities of the fluids are not the same, the density in a cell is approximated to be

$$\rho = \rho_c F + (1 - F) \rho_w \qquad (6)$$

From Eqs. (5) and (6), we see that the values of ν and ρ in a cell are functions of F.

Finally, it is noted that the Reynolds numbers based on the jet width and the velocities used in our computations are in the range of 20 - 2000. Within this range, Eqs. (2) and (3) are felt to be appropriate for the present flow analysis, even though the equations do not include turbulence considerations.

IV. COMPUTATIONAL RESULTS AND DISCUSSIONS. The following are the input data for the computations:

θ = incidence angle of the jet = 45^o

D_j = diameter of the jet (width of the jet in the two-dimensional model) = 1.83 mm

V_j = jet velocity, uniformly across the jet width = 5 - 12.5 m/sec

ρ_w = density of plain water = 0.001 Kg/cm^3

ρ_c = density of the contaminant = 0.00107 Kg/cm^3

ν_w = kinematic viscosity of water = 0.0098 cm^2/sec

ν_c = kinematic viscosity of the contaminant = 0.098 - 9.8 cm^2/sec

Contaminant Droplet With Initial Water Layer Coverage. This refers to the impingement flow developing from the configuration shown in Figure 1b. The two-fluid flow model of Figure 2 applies to this case. The velocities given above correspond to steady dynamic pressures of 2 - 12 psi, which are practical for decontamination. The dimension of the contaminant droplet is taken to be 3 mm x 0.6 mm, representing the average size on a horizontal flat surface. Two assumptions that have been made are that the contaminant droplet wets the wall and that the surface tension between the contaminant and the water can be neglected because it is small.

Before running the computer code SOLA-VOF [11] for the two-fluid flow, test runs of the code have been made to calculate the surface pressure upon an impingement of an incompressible, inviscid, normal jet. The result is in good agreement with Taylor's prediction. The following presents the results we have obtained so far in this research program.

Figure 5 shows the flow patterns following the commencement of the jet impingement. The jet flow comes in along the upper boundary above the left corner of the contaminant droplet. The small arrows in the flow channel represent the direction and the magnitude of fluid velocities at various points. In the left column of the figure, the viscosity of the water (including jet fluid and water layer) is ν_w = 0.0098 cm^2/sec (real value), while in the right column, ν_w has artificially been raised to the value of ν_c, i.e., ν_w = 0.98 cm^2/sec. The reason for raising the viscosity is to examine

the sensitivity of the flow to the variation of the viscosity of the jet fluid. A comparison between these two columns shows that the flow patterns corresponding to these two viscosity values are similar. Figure 6 presents another view of the evolution of the contaminant droplet. In the figure, the dash-line indicates the initial location of the upstream edge of the droplet and the distance S represents the displacement of the edge. This displacement can explicitly be used to evaluate the performance of a jet impingement flow for removal of contaminant droplets from a surface.

If the initial water layer above the contaminant droplet is reduced from 1 mm in Figure 5 to 0.2 mm presently, similarities also are obtained for the flow pattern and the displacement S when the two columns in Figure 7 are compared. Table I summarizes the results of the displacement S and the mean velocities $\dot{S}$ of the droplet upstream edge for two cases: $\nu_c = 0.98$ cm^2/sec and $\nu_c = 9.8$ cm^2/sec. The mean velocity here is defined as the value obtained by dividing the displacement S by the time after the commencement of the jet flow. We see that despite a dramatic variation of the jet fluid viscosity from $\nu_w = 0.0098$ cm^2/sec to $\nu_w = 9.8$ cm^2/sec, the difference of the resulting displacements S is of order of only 10 - 15%. In view of the large initial mean velocities, $\dot{S} > 3$ m/sec, listed in Table I, this magnitude of difference is considered insignificant since practically the droplet will be displaced almost immediately after application of the jet impingement. Therefore, the one-fluid flow model established in Section II is applicable to characterize the flow field developing from the configuration shown in Figure 1a. Physically, the insensitivity of the flow field to the variation of the jet fluid viscosity has demonstrated the dominance of the inertial force over the shear force. It should be noted, however, if the impingement location is far away from the contaminant droplet or if the initial water layer above the droplet is very thick, then the viscous effects of the jet fluid may not be ignored.

Contaminant Droplet Without Initial Water Layer Coverage. Now consider the flow configuration of Figure 1a for which the one-fluid flow model applies. Figure 8, obtained from the Tektronix Display Terminal, shows a series of flow developments following the initiation of the impingement. The jet stream first spreads out on the wall and then engages the contaminant droplet, and finally is lifted off the wall at some angle. The interface between the fluid and the contaminant is not shown in the figure since the one-fluid flow model is used, in which the two fluids have the same properties. However, using the technique of embedding Marker Particles which follow the fluid particles in the region initially covered by the contaminant droplet, we still are able to track the interface and observe its evolution. The result is shown in the first column of Figure 9. In the other columns of the figure, the results corresponding to higher viscosity values are presented. A comparison of these columns explicitly shows the viscosity dependence of the flow. It is seen that the viscosity smooths out the interface profile and resists the movement of the droplet. The latter effect can be seen in Figure 10. Another interesting result we have found is that even if the fluid viscosity is as small as 0.098 cm^2/sec (i.e., 10 times the viscosity of plain water) the downstream end of the droplet stil remains unchanged (shape and location) until a large portion of the droplet on the upstream side has been deformed or broken up.

Figure 11 shows the displacements S versus time corresponding to various jet velocities V_j. The origin of the time coordinate in the plot has been chosen to be the moment the droplet upstream edge starts to move. As anticipated, the jet velocity has proven to be an important parameter affecting the jet performance. Figure 12 is a plot of the mean velocity $\bar{v}$ versus the displacement S. With the fluid viscosity $\nu = \nu_w = \nu_c = 0.98$ cm^2/sec, it shows that as $v_j > 5$ m/sec, the droplet upstream edge can move with an initial velocity greater than 4.2 m/sec. As stated earlier, the velocity is large enough to displace the droplet almost immediately after jet impingement. Another important value we have to determine is the rise of pressure peak on the impingement surface. In some critical areas, such as the optical windows of a vehicle, the impact pressure that the areas can take is limited. Figure 12 presents some typical pressure distributions on the impingement surface as the jet-contaminant interaction flow continues to develop. As a result of transient phenomenon, the instantaneous pressure peak is seen to rise higher than twice the corresponding steady dynamic pressure of the jet velocity, $1/2\rho V_j^2$.

V. SUMMARY AND CONCLUSIONS. Two flow models have been developed to investigate the flow interaction of a liquid jet with a chemical contaminant droplet on a plane wall. If this situation is considered as a two-dimensional viscous flow, the result from the two-fluid flow model shows that the flow pattern is insensitive to the variation of the jet fluid viscosity. This leads to the feasibility of using the one-fluid flow model for characterizing the flow situation in which the contaminant droplet is not initially covered by a water layer.

The interfaces between fluids in the two-fluid flow and the free surface in the one-fluid flow can be tracked by computer simulations. Results from both models show that the downstream end of the contaminant droplet can remain unchanged (shape and location) until a large portion of the droplet on the upstream side has been deformed or broken up. The jet velocity and the viscosity of the contaminant are important variables affecting the flow field. The displacement and the mean velocity of the droplet upstream edge when subjected to a jet impingement can be calculated and can be used to evaluate the efficiency of the jet impingement for removal of the contaminant. It is found that with a jet velocity $V_j > 5$ m/sec, the impingement can displace the contaminant droplet almost immediately. The instantaneous pressure on the impingement surface may rise higher than twice the corresponding steady dynamic pressure of the jet velocity, $1/2\rho V_j^2$.

Further studies to establish correlations between flow parameters and the efficiency of the jet impingement for decontamination are in progress.

REFERENCES

1. G.I. Taylor, "Oblique Impact of a Jet on a Plane Surface," Phil. Trans. R. Soc. A, 260, 1966, pp. 96-100.

2. J.H. Michell, Phil. Trans. A, 181,1890, pp. 389-431.

3. M.T. Scholtz and O. Trass, "Stagnation Flow-Velocity and Pressure Distribution," AIChE J., 16, No. 1, Jan 1970, pp. 82-96.

4. A. Rubell, "Computations of Jet Impingement on a Flat Surface," AIAA J., 18, No. 2, Feb 1980, pp. 168-175.

5. A. Rubell, "Computations of the Oblique Impingement of Round Jets Upon a Plan Wall," AIAA J., 19, No. 7, Jul 1981, pp. 863-871.

6. D.R. Kotansky and W.W. Bower," A Basic Study of the VTOL Ground Effect Problem for Planar Flow," J. Aircraft, 15, No. 4, Apr 1978, pp. 214-221.

7. W.W. Bower, "Computations of Three-Dimensional Impinging Jets Based on the Reynolds Equations," AIAA Paper No. 82-1024, presented at the AIAA/ASME 3rd Joint Thermophysics, Fluids, Plasma, and Heat Transfer Conference, St. Louis, MO, 7-11 Jun 1982.

8. W.P. Jones and B.E. Launder, "The Prediction of Laminarization with a Two-Equation Model of Turbulence," Int. J. Heat and Mass Transfer, 15, 1972, pp. 301-314.

9. J.N. Hunt, "Wave Formation in Explosive Welding," 1967.

10. J-M Vanden-Broeck, "Deformation of a Liquid Surface by a Impinging Gas Jet," SIAM J. Appl. Math., 41, No. 2, Oct 1981, pp. 306-309.

11. B.D. Nicholas, C.W. Hurt, and R.S. Hotchkiss, "SOLA-VOF: A Solution Algorithm for Transient Fluid Flow with Multiple Free Boundaries," Los Alamos Scientific Laboratory Report No. LA-8355, 1980.

Table I. Displacements and Mean Velocities of Contaminant Droplet Upstream Edge After Initiation of Jet Flow

$\nu_c = 0.98\ cm^2/sec$

V_j m/sec	Time MS	$\nu_w = 0.98 cm^2/sec$		$\nu_w = 0.0098 cm^2/sec$		$\frac{S_2 - S_1}{S_2}$ %
		S_1 mm	$\dot{S}_1$ m/sec	S_2 mm	$\dot{S}_2$ m/sec	
5	0.05	0.207	4.13	0.214	4.28	3.4
	0.10	0.122	4.22	0.436	4.36	3.2
	0.15	0.552	3.68	0.597	3.98	7.5
10	0.05	0.467	9.3	0.52	10.04	10.2
	0.10	0.624	6.24	0.727	7.27	14.1
	0.15	0.642	4.28	0.761	5.07	15.6

$\nu_c = 9.8\ cm^2/sec$

V_j m/sec	Time MS	$\nu_w = 9.8 cm^2/sec$		$\nu_w = 0.0098 cm^2/sec$		$\frac{S_2 - S_1}{S_2}$ %
		S_1 mm	$\dot{S}_1$ m/sec	S_2 mm	$\dot{S}_2$ m/sec	
5	0.05	0.150	3.04	0.17	3.42	11.1
	0.10	0.280	2.80	0.32	3.20	12.5
	0.15	0.409	2.73	0.445	2.97	8.1
10	0.05	0.257	5.14	0.305	6.10	16.0
	0.10	0.510	5.10	0.580	5.80	12.1
	0.15	0.54	3.60	0.620	4.13	13.0

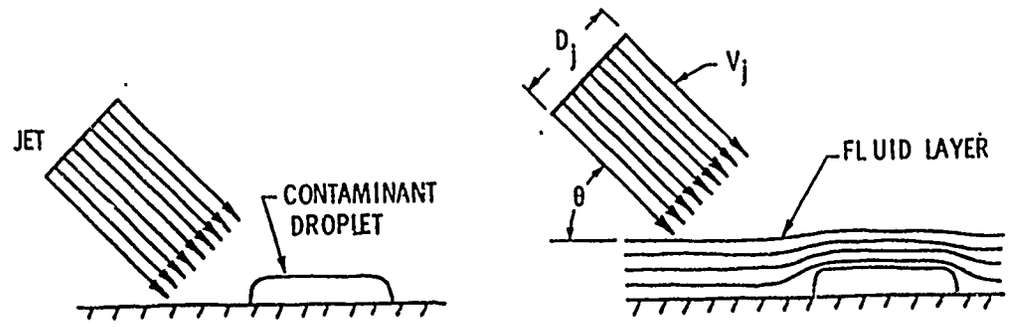

a. Contaminant Droplet Without Initial Fluid Layer Coverage

b. Contaminant Droplet With Initial Fluid Layer Coverage

Figure 1. Pre-impingement Flow Configurations

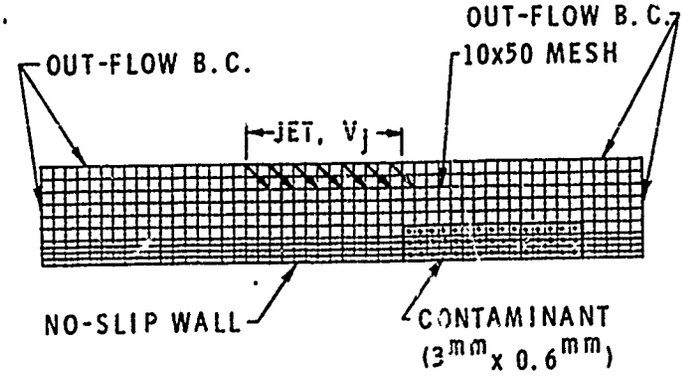

Figure 2. Two-Fluid Flow Model

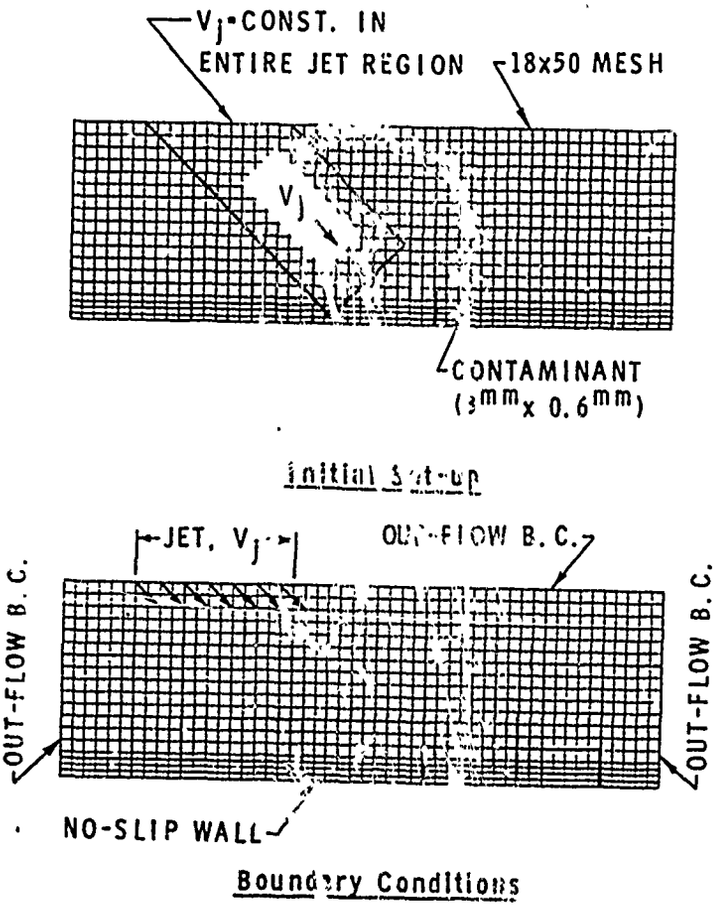

Figure 3. One-Fluid Flow Model

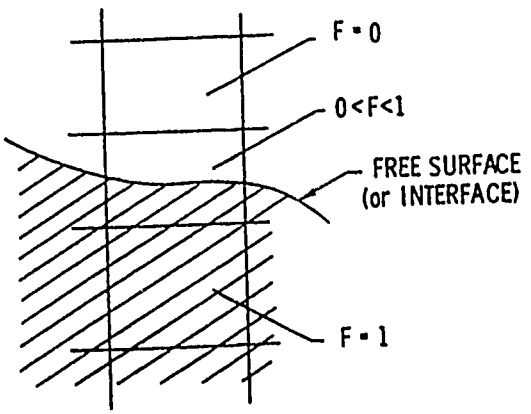

Figure 4. Interface Between Two Fluids
(or Free Surface of One Fluid)

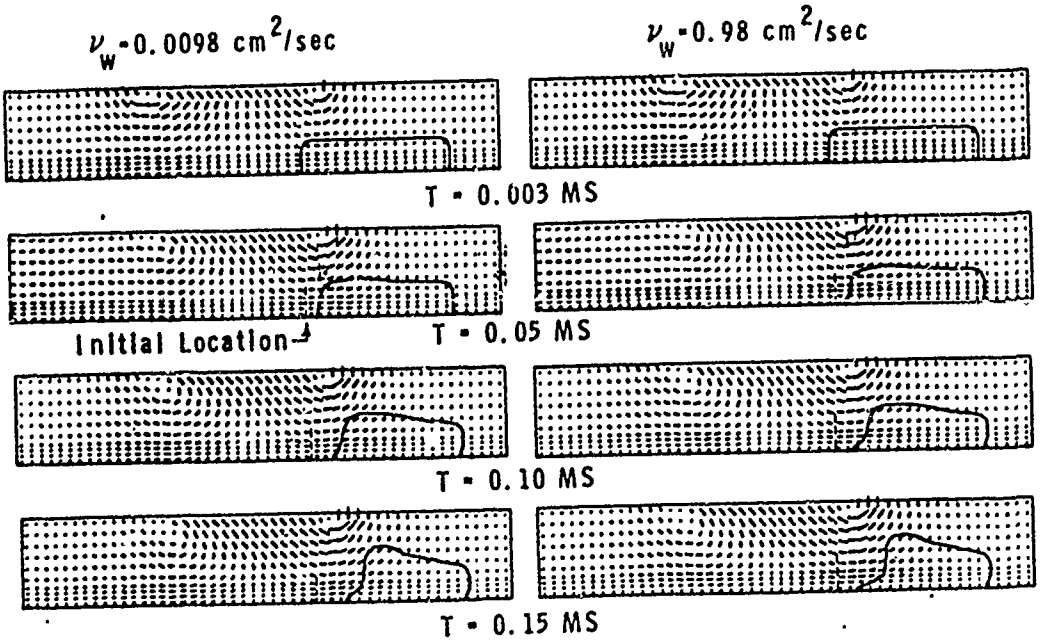

Figure 5. Flow Patterns (Two-Fluid Flow, ν_c = 0.98 cm^2/sec, V_j = 10 m/sec, $\theta = 45^o$)

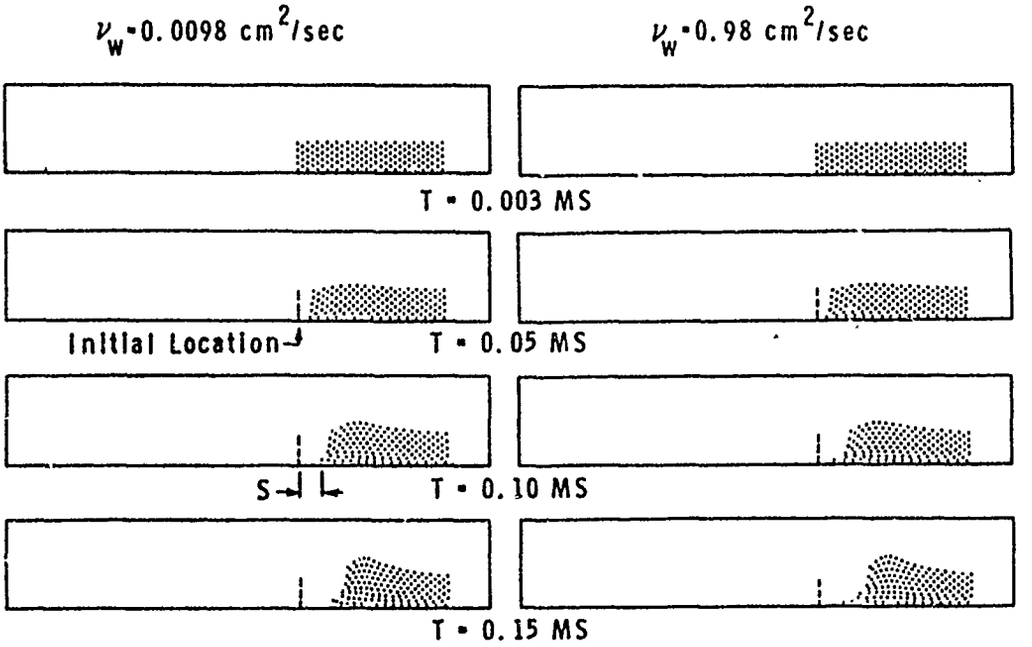

Figure 6. Evolution of Contaminant Droplets (Two-Fluid Flow, ν_c = 0.98 cm^2/sec, V_j = 10 m/sec, θ = 45°)

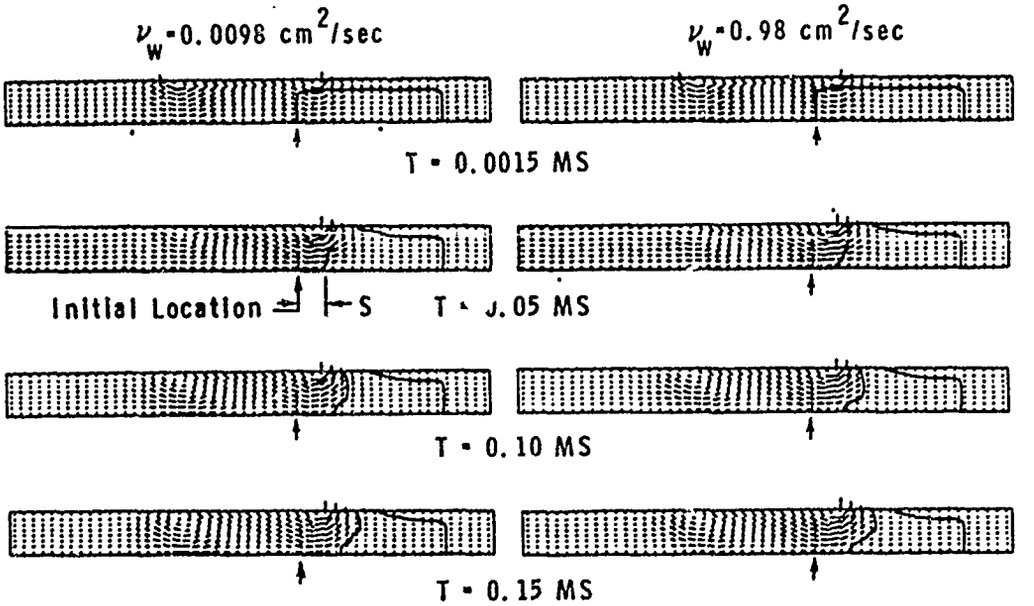

Figure 7. Flow Patterns (Two-Fluid Flow with Reduced Thickness of Initial Fluid Layer Coverage, ν_c = 0.98 cm^2/sec, V_j = 10 m/sec, θ = 45°)

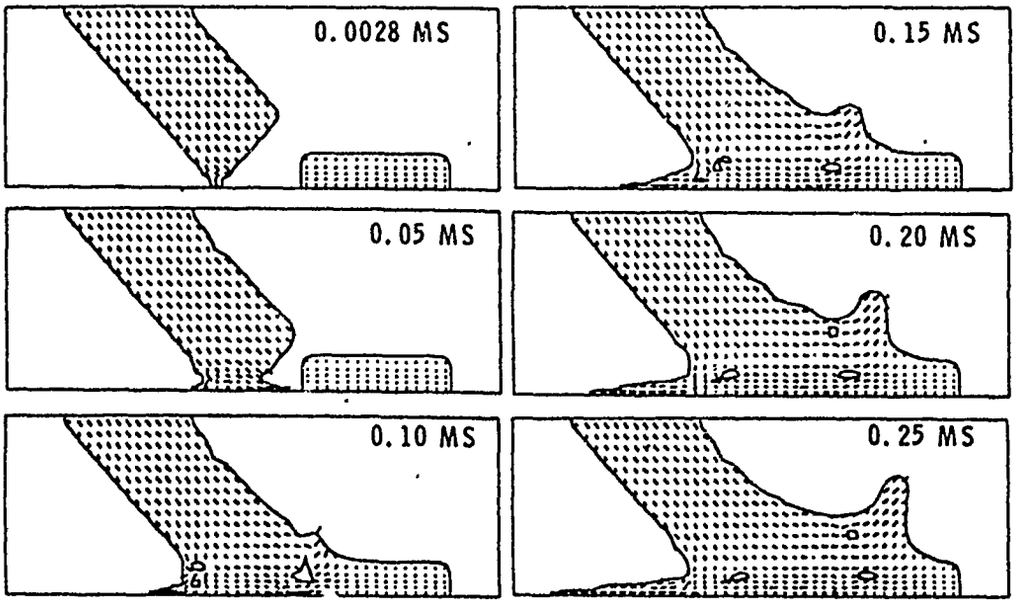

Figure 8. Flow Patterns (One-Fluid Flow, $\nu_c = \nu_w = \nu = 0.098$ cm^2/sec, V_j = 10 m/sec, $\theta = 45^o$)

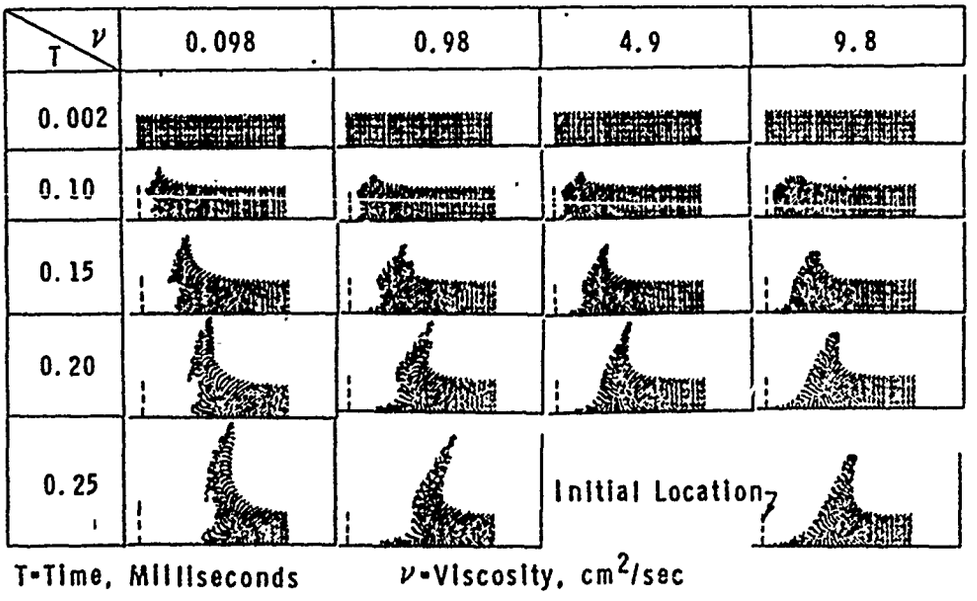

Figure 9. Evolution of Contaminant Droplets Resulting from Various Viscosities (One-Fluid Flow, V_j = 10 m/sec, $\theta = 45^o$)

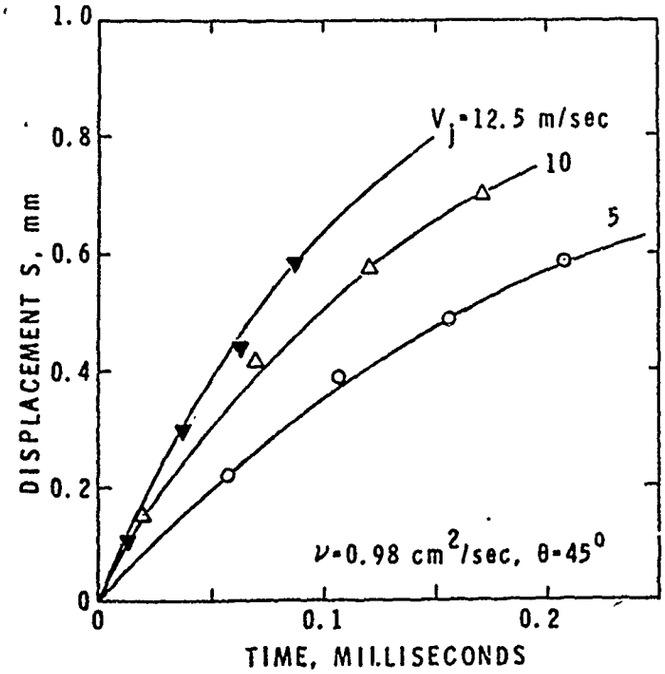

Figure 10. Contaminant Droplet Upstream Edge Displacement Vs. Time after the Edge Starts to Move

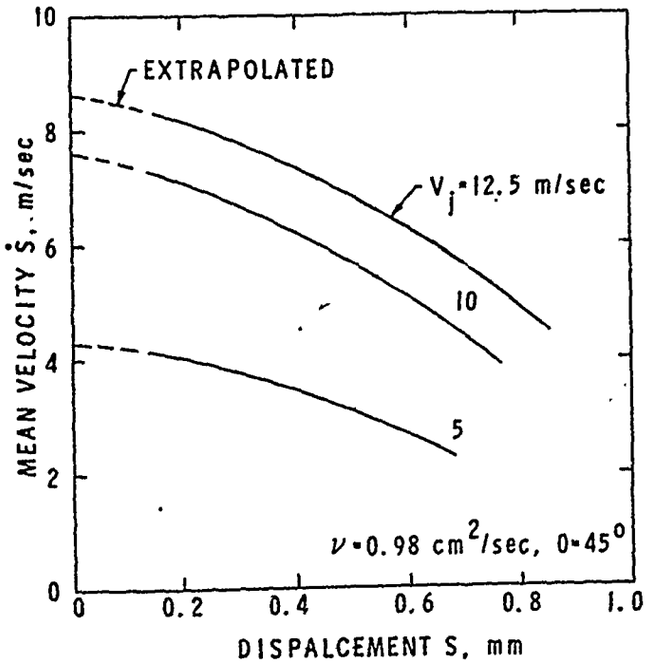

Figure 11. Mean Velocity vs. Displacement of Contaminant Droplet Upstream Edge

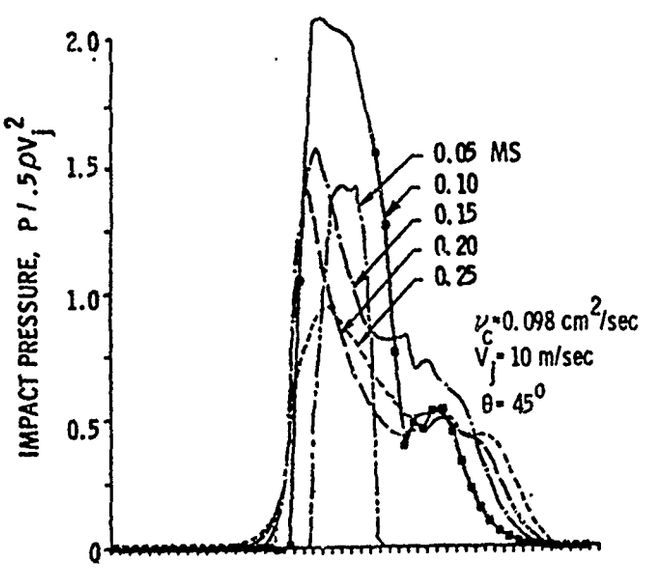

Figure 12. Pressure Distributions on Impingement Surface after Initiation of Jet Flow